GCU
Glasgow Caledonian
University

University for the Common Good

Monitoring contamination level on insulator materials under dry condition with a microwave reflectometer

Jiang, Y.; McMeekin, S.G.; Reid, A.J.; Nekahi, A.; Judd, M.D.; Wilson, A.

Monitoring Contamination Level on Insulator Materials under Dry Condition with a Microwave Reflectometer

Y. Jiang, S. G. McMeekin, A. J. Reid, A. Nekahi
Glasgow Caledonian University
School of Engineering and Built Environment
Glasgow, G4 0BA, United Kingdom

M. D. Judd
High Frequency Diagnostics and Engineering Ltd
Glasgow, G52 3NU, United Kingdom

A. Wilson
Doble PowerTest Ltd
Surrey, GU3 1NA United Kingdom

ABSTRACT

Current techniques used for monitoring the levels of contamination on high voltage insulators, such as leakage current and infrared, are not effective in dry conditions since they require the surface of the insulator to be wetted by fog, rain or snow. If a buildup of contamination occurs during a prolonged dry period prior to a weather change there will be a significant risk that flashover may occur before there is time to implement preventative maintenance. Previous work has demonstrated the use of microwave radiometry to determine the levels of contamination on an insulator material under dry conditions, however practical applications are limited by low sensitivity. This paper reports the development of a novel technique based on microwave reflectometry to detect the power levels reflected from the surface of the insulator material. The level of contamination is then determined as a function of received power. A theoretical model establishes the relationship between equivalent salt deposit density levels on insulator surface and the dielectric properties of the contamination layer. A Finite Difference Time Domain (FDTD) model is used to simulate the total loss as a function of the contamination level. Experimental results verify the FDTD model and demonstrate the sensitivity of the reflectometer system to be approximately 100 times greater than the radiometer system. Therefore, the reflectometry system has considerably greater potential for practical applications to provide advance warning of the future failure of insulators under dry conditions for both HVDC and HVAC systems.

Index Terms — Insulators, Microwave reflectometry, Insulator contamination, Pollution measurement

1 INTRODUCTION

HIGH Voltage (HV) insulators are a key component in AC and DC transmission and distribution lines and substations. The build of a contamination layer on the insulator can lead to flashover resulting in failure of the network and power outage. The ability to monitor the buildup contamination could provide an important aid to implement an effective preventative maintenance scheme.

CIGRE working group, C4.303, reported that build-up of contamination on the insulator surface of High Voltage Direct Current (HVDC) insulation can be up to 10 times more severe than that on comparable High Voltage Alternating Current (HVAC) insulation under the same environment. This was attributed to charge build up not being cancelled by polarity reversals on HVDC insulator resulting in more aggressive arcing during the formation of the dry-bands [1]. The recent growth in HVDC networks therefore makes the development of an effective monitoring system for contamination levels more imperative.

The severity of the pollution is determined in term of both equivalent salt deposit density (ESDD) which contributes to electrical conduction and non-soluble deposit density (NSDD) which contributes to water retention [2]. Because the contamination has low conductivity under dry condition, it is usually less significant to the insulation level. However, after the surface is wetted by rain, snow, fog or dew, the

contaminants dissolve to form a conductive layer on the insulator surface thereby initiating leakage current and dry-band arcing, and which can ultimately lead to flashover [2-4].

In order to keep the contamination under control, a variety of condition monitoring techniques have been developed for both on-line and off-line measurements. The standard method given by IEC 60815 is the direct reading of ESDD and NSDD by cleaning the insulator in a specific volume of water [5]. However, this method requires the insulator to be taken off-line. For on-line monitoring, most countries determine the pollution severity based on leakage current or electrical field [6-8]. These conventional monitoring systems have several drawbacks:

a. The systems have only been studied and tested for HVAC system. The application of these systems for HVDC system is limited where the contamination problem has been reported to be 10 times more severe than HVAC system [1, 9].

b. Both leakage current and electrical field monitoring systems are only effective when the contamination layer has been wetted by rain, fog or condensation; under these conditions flashover might occur before there is time to implement remedial measures such as cleaning [10].

c. The outputs of these systems are hard to convert to ESDD and NSDD which directly present the pollution severity.

To address these problems, the authors have previously reported a novel method based on microwave radiometer for monitoring high voltage insulator contamination level [20, 21]. The microwave radiometer system demonstrated its potential to detect different levels of contamination on insulator material under dry conditions without any physical contact with insulation system. However, the radiometer system suffers from low sensitive and interference. This paper suggests another novel method that builds on the radiometer system by using microwave reflectometry to achieve higher sensitive and less susceptible to interference. As a non-invasive technique, microwave reflectometry is used for analysing the properties of a medium. It has been widely used in radar, oceanography, non-destructive testing and medical imaging [11]. The technique is based on a transmitter that generates a radio frequency (RF) signal. The RF signal is reflected at the interface of interest and the reflected signal is detected by a receiver. Properties of the reflected signal such as magnitude, time delay and power level contain the information concerning the object under test. In this paper, the power level of the reflected signal is investigated. The contamination layer on a polluted insulator reflects a different electromagnetic energy level compared to a clean insulator under the same microwave illumination. Thus, the contamination level on an insulator surface can be determined by measuring the received power level of the reflected signal [12]. It could be developed to a safe, reliable condition monitoring method for both HVDC and HVAC system, which is effective under dry conditions at a reliable long distance.

To remove the effect of the complex surface geometry of the HV insulators for testing the concept, it was decided to develop an initial theoretical model and an associated experiment using a flat plane. The paper presents a theoretical model for determining the relationship between ESDD levels on insulator surface, dielectric properties of the contamination layer, geometry and the total loss of the polluted sample. The total loss, which represents the ratio between reflected power and transmitted power is simulated by a finite difference time domain (FDTD) model. To verity the theories, a 10.45 GHz microwave reflectometer was specifically designed with high sensitivity and stability and with relatively low cost and then tested under dry conditions.

2 THEORETICAL MODEL

Microwave reflectometer techniques are widely used in soil moisture and salinity measurement for determining dielectric properties and work has been published on the use of models to measure the dielectric properties of multi-layer materials [13-15]. Obtaining the ESDD of a contamination layer can be treated in a similar manner to the soil salinity detection problem with multiple layers. In a microwave reflectometer system the total loss describes the reduction in power density of an electromagnetic wave as it propagates through the object under test. The material properties of the contamination layer and the system geometries will affect the total loss. Material properties include the complex dielectric constant and permeability of the contamination, which are related to ESDD. The dielectric properties of the material involve several unknown parameters including moisture, salinity, bulk density, thickness and surface roughness. The contamination layer on an insulator is relatively thin with a smooth surface, therefore the influence of thickness and surface roughness can be ignored when compared to moisture and salinity. The bulk density is calculated based on the properties of the artificial contamination layer described in IEC 60507 [16]. With these simplifications, the only parameters that need to be inferred are moisture and salinity.

Figure 1 shows the proposed system model relating the total loss of the reflectometer to the ESDD on insulator surface. Within this framework, the dielectric mixing model evaluates the complex permittivity and permeability of insulator contamination layer as a function of moisture, salinity, environment temperature and humidity by assuming it is salt and water affected soil. The FDTD
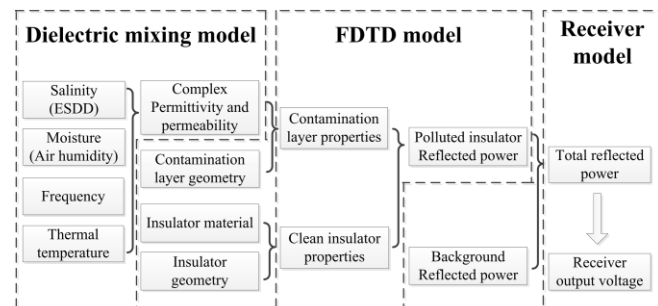

Figure 1. Theoretical model of applying reflectometry to monitor insulator contamination.

model evaluates propagation of the electromagnetic wave through the complex geometries of antennas, insulator and contamination layer. Finally, the receiver model calculates the system total loss by the output voltage of the receiver which is inversely proportional to the reflected power.

2.1 DIELECTRIC MIXING MODEL

The objective of the dielectric mixing model is to determine the complex permittivity and permeability of the contamination layer. The model to calculate the complex permittivity was developed in previous work reported by the authors on microwave radiometer [12, 17, 18]. In this paper, only the main steps of the dielectric mixing model are presented for clarity in the development of the complete microwave reflectometry model.

The real and imaginary parts of the complex permittivity of saline water, derived from a formulation given by Stogryn, are respectively given by [19-21]:

$$
\begin{cases}
\varepsilon'_{sw} = \varepsilon_{sw\infty} + \dfrac{\varepsilon_{sw0} - \varepsilon_{sw\infty}}{1 + (2\pi f \tau_{sw})^2} \\
\varepsilon''_{sw} = \dfrac{2\pi f \tau_{sw}(\varepsilon_{sw0} - \varepsilon_{sw\infty})}{1 + (2\pi f \tau_{sw})^2} + \dfrac{\sigma_{NaCl}}{2\pi \varepsilon_0 f}
\end{cases} \tag{1}
$$

where $\varepsilon_{sw\infty} = 4.9$ is the high frequency limit of ε'_{sw} and $\varepsilon_0 = 8.854 \times 10^{-12} (\text{F/m})$ is the permittivity of free space. According to IEC 60507 [16], the saline water in the insulator contamination layer can be represented as NaCl solution.

Equation (2) below, developed by Dobson [22], represents the dielectric constant of soil as a function of soil moisture, m_v, dielectric constant of pure water inside soil, ε_{pw}, permittivity of dry soil, ε_s, bulk density of dry soil, ρ_s and bulk density of wet soil, ρ_b.

$$
\begin{cases}
\varepsilon'_m = (1 + (\rho_b/\rho_s)\varepsilon_s^\alpha + m_v^{\beta'} \varepsilon'^\alpha_{pw} - m_v)^{\frac{1}{\alpha}} \\
\varepsilon''_m = (m_v^{\beta''} \cdot \varepsilon''^\alpha_{pw})^{\frac{1}{\alpha}}
\end{cases} \tag{2}
$$

where α and β are related to the soil texture. By combining equation (2) with Stogryn's model given in equation (1), the dielectric constant of pure water is replaced with the dielectric constant of saline water where $\varepsilon'_{pw} = \varepsilon'_{sw}$ and $\varepsilon''_{pw} = \varepsilon''_{sw}$. In IEC 60507, the contamination layer consists entirely of Kaolin, which is a form of clay with a typical bulk density of $\rho_b = 1$ g/cm^3.

The complex permeability of the contamination can be expressed by:

$$
\mu_m = 1/(\mu_0 \varepsilon_0 \varepsilon_m v_p^2) \tag{3}
$$

Where v_p is the phase velocity of light; $\varepsilon_m = \varepsilon'_m - j\varepsilon''_m$ is the complex permittivity of the contamination layer in equation (2) and μ_0 is the permeability of free space.

Figure 2 shows the relationship between the complex permittivity, moisture (M in percentage), salinity and observation frequency from the dielectric mixing mode.

According to the Figure 2, moisture and salinity affect both the real and imaginary part of the complex permittivity while the real part is more sensitive to the change of the water content and the imaginary part is more sensitive to the change of the salinity. The complex permittivity is more sensitive to salinity in the lower frequency range [23]. However, a lower observation frequency has a longer wavelength as shown in the equation $\lambda = v_p / f$, which leads to poorer spatial resolution. With poor spatial resolution, electromagnetic wave can easily propagate over the test samples by diffraction. In order to achieve a balance between system sensitivity and spatial resolution a frequency of 10.45 GHz was selected, with a wavelength of 28.7 mm this compares with the size of the insulation sample 500 mm $\times$ 200 mm, was chosen for further studies.
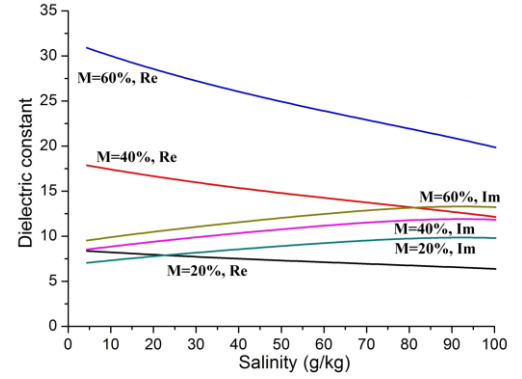

Figure 2. Theoretical relationship between complex dielectric constant, moisture, frequency and salinity at 10.45 GHz.

2.2 FDTD MODEL

A 3-dimensional Finite Difference Time Domain (FDTD) model was developed to simulate the electromagnetic propagation from transmitter to receiver and to study the relationship between the reflected power from the contaminated surface of the insulator and the material properties of the contamination layer. The FDTD simulation will also enable models for more complex geometrical representations of the insulator with contamination layer to be developed in future. The present study replaced the complex geometrical shape of the sheds on a HV insulator with a flat insulator of dimensions of 500 mm $\times$ 200 mm and 8 mm thickness. This enabled the proposed FDTD model to be verified independent of the geometry of the insulator.

The FDTD model was based on the arrangement shown in Figure 3. The sample is covered with a 0.3 mm thick homogeneous contamination layer and two X-band horn antennas are placed to point to the flat sample with an angle θ, as shown in Figure 3.
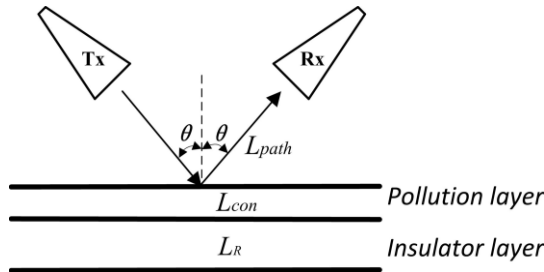
Figure 3. Geometry of the FDTD model, Tx: transmitter, Rx: Receiver, L_{path}: path loss from transmitter to receiver, L_{con}: loss on pollution layer, L_R: loss on insulator sample.

A 10.45 GHz sinusoidal signal is injected at the transmitter horn antenna, Tx, shown in Figure 3, while the received power at the receiver horn antenna, Rx, is recorded by a plane sensor. The sample is placed 600 mm away along and with its center on the boresight of the antennas. The power level at the receiver will be dependent upon the losses associated with L_{path}, L_R and L_{con}.

The material properties used for the contamination layer were the complex permittivity and permeability calculated by dielectric mixing model at 10.45 GHz with 6 different ESDD levels under dry conditions. The insulator plane was assigned constant permittivity and permeability of glass or porcelain as show in Table 1 [24, 25]. The antennas were treated as perfect electrical conductors. All the boundaries were defined using absorbing boundary conditions to eliminate unwanted microwave reflections into the region of interest. Each simulation ran 40 ns with 4 ps time step.

Table 1. Permittivity and permeability of insulator material at 10.45 GHz.

Material	ε'	$tan\delta_\varepsilon$	μ'	$tan\delta_\mu$
Glass	4.2	0.00058	1.13	1.15
Porcelain	2.09	0.00004	1.06	1.02

Figure 4 shows the simulated power received when $\theta = 30°$ and ESDD level is 0.12 mg/cm^2. It shows that the wave travels from the transmitter to sample and finally reaches the receiver after 5 ns. The received signal takes another 15 ns to stabilize. The output of the receiver is proportional to the average power after the system becomes stable.
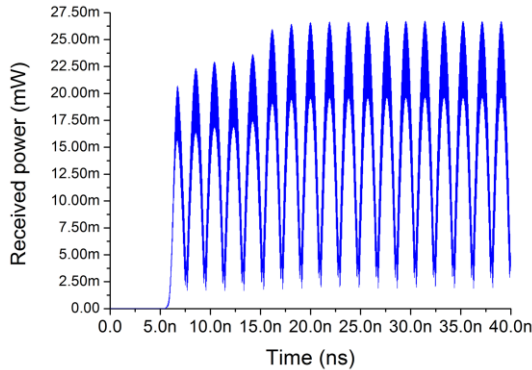

Figure 4. Power received by the receiver antenna of the FDTD simulation (glass sample, $\theta = 30°$, ESDD = 0.12 mg/cm^2).

Figure 5 shows the relationship between the total loss and the ESDD (from 0 to 0.12 mg/cm^2 with 0.02 mg/cm^2 step) calculated by the FDTD simulation for $\theta = 30°$. The
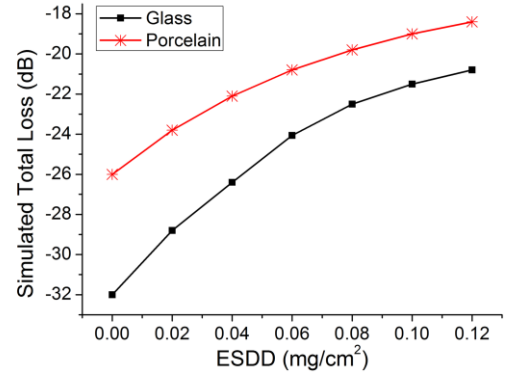

Figure 5. Simulated total loss, L''_{tot} (dB), as a function of ESDD level for glass and porcelain substrates calculated by the FDTD simulation for $\theta = 30°$.

total loss in the simulations, L''_{tot}, is defined as the ratio of transmitted power, P''_t, to the received power, P''_r, as given by:

$$L''_{tot} (dB) = 10log_{10}\frac{P''_t}{P''_r} \qquad (4)$$

Note that all simulated variables in this paper are decorated with double prime symbol, $''$, to differentiate from the experimental variables. The results show that the different ESDD levels can be clearly distinguished. After using a receiver circuit to detect the power received by antenna and calculate the total loss, the reflectometry may therefore be able to detect different ESDD levels under dry conditions.

3 REFLECTOMETER SYSTEM

3.1 REFLECTOMETER DESIGN

A schematic diagram of the transmitter and receiver circuits used for the microwave reflectometer are shown in Figure 6. The transmitter used for the experiment is an X-band horn antenna with 20 dB gain and 16.5° beam width directly connected to a 10.45 GHz Gunn oscillator with +13 dBm output power. The receiver is a power detector with a superheterodyne architecture. After the receiver horn antenna, a low noise amplifier (LNA) amplifies the signal and a bandpass filter selects the 10.45 GHz signal prior to the downconverter and low-frequency circuit. The superheterodyne circuit contains a mixer and a 10.65 GHz local oscillator. It downconverts the 10.45 GHz input signal
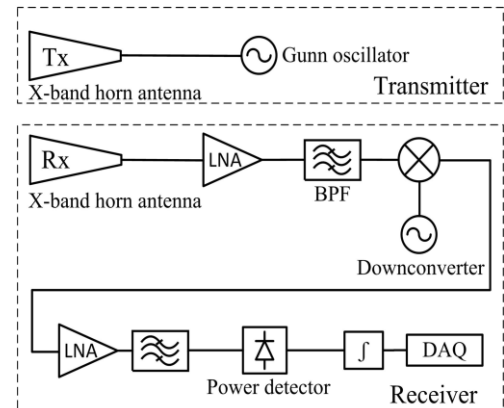

Figure 6. Transmitter and receiver circuits.

to a 200 MHz signal. The LNA and a bandpass filter at this frequency further improve the signal-to-noise ratio before a square-law power detector provides a dc output voltage that is inversely proportional to the input power.

3.2 CHARACTERISATION OF SYSTEM OUTPUT AS A FUNCTON OF TOTAL LOSS

In order to establish the relationship between the output voltage from the microwave radiometer and the properties of the contamination layer on the insulator surface, as determined by the FDTD model, it is necessary to calibrate the system in terms of the overall total loss.

The dc output voltage of the power detector, shown in Figure 6, is given by:

$$V_{det} = K_{det}G_{RF}(P_r + P_{Cn}) + C_{det} \tag{5}$$

where K_{det} and C_{det} are the gradient and offset of the power detector; G_{RF} is the gain of radio frequency (RF) circuit, P_r is the received power of the antenna and P_{Cn} is the power due to noise generated by the circuit components. The dc output voltage is amplified and filtered by a low frequency (LF) circuit and the final output voltage at the DAQ is given by:

$$V_{out} = G_{LF}(V_{det} - V_{dc}) \tag{6}$$

where G_{LF} and V_{dc} are the low frequency gain and dc offset of LF circuit. By substituting (5) into (6), the output voltage as a function of the received power is given by:

$$\begin{cases} V_{out} = GP_r + C \\ G = K_{det}G_{RF}G_{LF} \\ C = G_{LF}(K_{det}P_{Cn} + C_{det} - V_{dc}) \end{cases} \tag{7}$$

In the experiment, G and C are constants defined by the gain and voltage offset of the circuit. The only variable is the received power P_r:

$$P_r = P_t L_{tot} + P_{Rn} \tag{8}$$

where P_t is the transmitted power, P_{Rn} is the external noise from the surrounding environment and L_{tot} is the total loss due to the propagation path from transmitter to receiver, L_{path}, the reflection loss from the insulator material sample plane, L_R, plus an additional loss due to the contamination layer on the insulator surface, L_{con}, (as shown in Figure 3):

$$L_{tot} = L_{path} + L_{con} + L_R \tag{9}$$

L_{con} is the only variable that is dependent upon the properties of the contamination layer on the insulator surface. A reference sample is tested at regular intervals during measurement in order to remove the effect of the variables P_{Cn}, P_{Rn}, L_R and L_{path}, The reference sample has the same geometry and properties as the test sample but no contamination layer. The received power from the reference sample, P_{r_ref}, is:

$$P_{r\_ref} = P_t L_{ref} + P_{Rn} \tag{10}$$

where $L_{ref} = L_{path} + L_R$. Thus, the output voltage difference between the test sample and the reference is:

$$V_{diff} = V_{out} - V_{out_{ref}} = G(P_r - P_{r\_ref})$$
$$= GP_t L_{con} \tag{11}$$

Thus, the loss due to the contamination layer in the experiment can be calculated by equation (12),

$$L_{con} = V_{diff}/G_f \tag{12}$$

where $G_f = GP_t$ is a constant which is determined by the circuit components and the transmitted power. In the FDTD model, the loss due to the contamination layer, $L_{con}^"$, can be calculated by:

$$L_{con}^" = L_{tot}^" - L_{ref}^" = (P_r^" - P_{r\_ref}^")/P_t^" \tag{13}$$

where $P_{r\_ref}^"$ is the received power of the reference sample in the FDTD model. For the purpose of testing the concept, the effectiveness of this method can be verified if experimental loss due to the contamination layer, L_{con}, agrees with the simulated value, $L_{con}^"$.

4 EXPERIMENT

4.1 SAMPLE PREPRATION

The solid layer method recommend in IEC 60507 was employed to form an artificial pollution layer on the sample surfaces. This method involves uniformly spraying a pollution suspension through nozzles of a commercial type spry gun with 30 cm distance on the sample surfaces to form a solid layer [16]. The composition of the suspension used in tests contained 6.5 g Kaolin, 150 g water and a suitable amount of NaCl to control the ESDD level. A 150 ml suspension was sprayed evenly on one sample surface and the sample was then left to dry for 48 hours in a low humidity room. After the test had been completed, the solid layers were washed off by a clean cloth with 500 ml distilled water and the ESDD of each sample was obtained by measuring the conductivity of the washing water and then calculated using equation (14) [2]:

$$\begin{cases} ESDD = S_a \cdot V/A \\ S_a = (5.7 \cdot \sigma_{20})^{1.03} \end{cases} \tag{14}$$

where S_a is the salinity, σ_{20} is the conductivity of the NaCl solution corrected to 20 ℃, V is the volume of distilled water and A is the sample surface area.

Six pairs of glass and porcelain samples were tested, each with different contamination levels. Table 2 lists the properties of the contamination layers on these sample pairs.

Table 2. Properties of the contamination layers on 6 sample pairs.

Sample pair	NaCl (g)	ESDD on glass (mg/cm²)	ESDD on porcelain (mg/cm²)
1	3	0.0221	0.0211
2	6	0.0440	0.0413
3	9	0.0610	0.0582
4	12	0.0797	0.0746
5	15	0.1051	0.0952
6	18	0.1221	0.1125

4.2 EXPERIMENTAL SETUP

Both samples and antennas were fixed with specially designed clamps to minimize any difference in the positioning of the samples relative to the antenna. Figure 7 shows the system setup. The reflectometer was packaged inside a metal box to avoid external RF noise and allowed to stabilize for 30 minutes, to achieve thermal stability
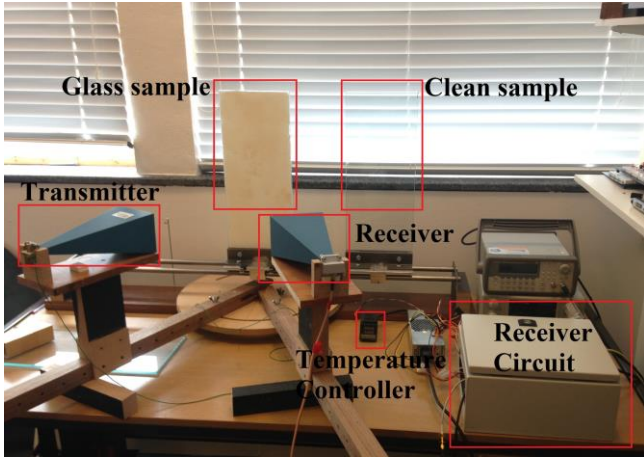
Figure 7. Experimental setup of the reflectometer system.

within the system, before any measurements were recorded.

The output voltage for each sample was averaged over 30 measurements to reduce experimental variation and to study the repeatability of the measurements. For each measurement, the reflectometer outputs were recorded with the system integration time of 1 second to provide a single dc value. After each measurement, the reference sample was tested and its output voltage was recorded to monitor the system stability.

4.3 RESULTS

Figure 8 shows the typical output voltages of the reflectometer system when testing clean, light polluted and heavy polluted samples. The results clearly show significant varying dc offset in the output voltages for the varying levels of contamination with an approximate 350 mV difference between the heavy polluted samples and the reference. The reference sample shows the best stability with the variation in the output voltage of less than ± 1% while the voltage output from the heavy polluted sample has a variation of 25%. The change in variation between the samples may be attributed to the rougher surface of the sample with higher ESDD.
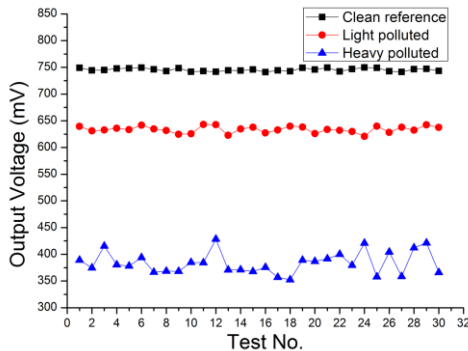

Figure 8. Output voltage of the reflectometer for different pollution levels.

Figure 9a shows the L_{con} calculated using equation (12) and the $L_{con}^{"}$ calculated using equation (13). It shows good agreement between the theoretical model and the experimental results for glass samples while the L_{con} was increasing with the ESDD level. The error bars of experimental results show the variation in measurement

taken over the results from 30 repeated tests. Although there were overlaps of the error bars between the neighbouring samples, the average results could be used to distinguish the ESDD levels clearly. There are several reasons that cause the disagreement between the theoretical model and the experimental results. Firstly, the G_f in equation (12) was calculated by using the circuit properties from the datasheet which may have the errors between the practical values. Secondly, for lower ESDD level, the solution with little NaCl was hard to form a uniform contamination layer. The most seriously, for higher ESDD level, the crystallization of the high salinity solution made uneven surface of the contamination layer. It greatly increased the surface roughness and the scattering of the surface became no longer negligible. Besides, external RF interference inside the passband of the filter may be strong enough to bring in some small noise. The results were similar on the porcelain samples, with Figure 9b showing good agreement between the theoretical model and the experimental results. Compared with the glass samples, the system presents lower sensitivity of the ESDD levels.
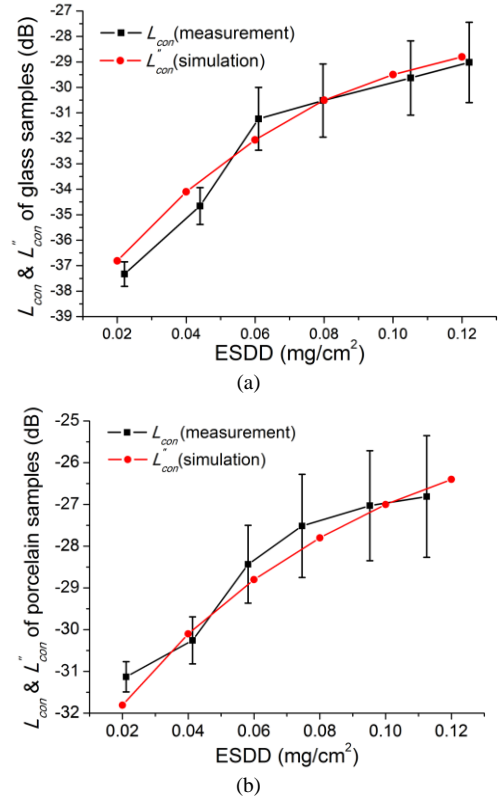

(a)

(b)

Figure 9. Experimental measurements and FDTD simulation of the L_{con} and $L_{con}^{"}$ as a function of ESDD levels for (a) glass, and (b) porcelain samples.

Figure 10 shows the comparison of the sensitivity of the output voltages to changes in ESDD levels for both the reflectometer and the radiometer systems [21]. The sensitivity is defined as the change in output voltage in mV for a change in ESDD level of 1 mg/cm². Identical receiver circuits were used for both systems to ensure the same level of gain. Both systems have demonstrated the ability to detect pollution levels under dry condition. However, as can be seen in Figure 10, the sensitivity of the reflectometer

system is approximately 100 times greater than the radiometer system with values of 4750 mV/(mg/cm^2) and 50 mV/(mg/cm^2) respectively. In addition, the reflectometer system is shown to be more stable under harsh environments and less susceptible to background EM interference since the power levels reflected from the insulator surface are significantly higher than the background levels of EM interference. Although the reflectometer has more complex circuit and requires an additional source, it is a more practical method for monitoring insulator contamination level compare to the radiometer system.
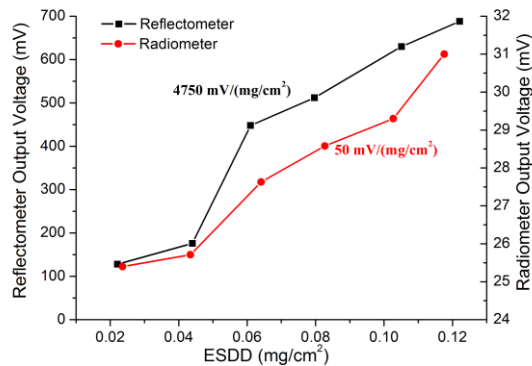

Figure 10. Comparison of the system outputs achieved by the radiometer and reflectometer systems.

5 CONCLUSION

This paper has described a theoretical and experimental study into the feasibility of using a 10.45 GHz reflectometer to assess contamination levels on HV insulators under dry conditions. The theoretical model employs the principles of remote sensing techniques and uses an FDTD model to evaluate the relationship between the contamination layer equivalent salt deposit density levels, complex dielectric properties and the total loss. A 10.45 GHz transceiver was designed and implemented to measure the power reflected from the surface of the polluted sample. The samples were polluted based on IEC standard 60507. The experimental results show good agreement with the theoretical model and validate the proposed method under dry conditions. According to the experimental results, this novel method is effective under dry conditions and has a more sensitive response to contamination on a glass surface rather than a porcelain surface. The system sensitivity has been greatly improved compared to the radiometer system previously reported by the authors. By using a transmitter instead of receiving passively, the system has strong anti-interference ability.

The maximum working distance between the antenna and insulator will be determined by the size of the insulator and the antenna beamwidth. For the experimental set up presented in this paper, the maximum working distance was approximately 1 meter by using horn antennas with 16.5° beamwidth. By using directional antennas with narrower beamwidth the maximum working distance could be increased, for example a reduction to beamwidth of 3°

would increase the theoretical working distance to over 6 meters.

The work provides a foundation for future investigations into the development of an on-line monitoring system for insulator pollution that is effective under dry conditions and the both HVDC and HVAC systems.

In future, the effects of non-soluble salt deposit density and the scattering of the rough polluted surface will be studied. The system will be also tested for monitoring energized insulators to evaluate any potential effect of the electric field around insulator. Additional frequency bands may also be employed to increase the accuracy. More advanced FDTD models for insulators with more complex geometries and materials will also be necessary to simplify the conversion of the L_{con} to the ESDD levels.

ACKNOWLEDGMENT

REFERENCES

[1] CIGRE Working Group C4.303, "Outdoor Insulation in Polluted Conditions: Guidelines for Selection and Dimensioning Part2: The DC Case", CIGRE, 2012.

[2] M. Farzaneh and W. A. Chisholm, *Insulators for Icing and Polluted Environments*, Wiley-IEEE Press, 2009.

[3] Lightning and Insulator Subcommitte, "Application of Insulators in a Contaminated Environment," IEEE Trans. Power App. Syst, vol. PAS-98, pp. 1676-1695, 1979.

[4] S. Venkataraman and R. S. Gorur, "Prediction of flashover voltage of non-ceramic insulators under contaminated conditions", IEEE Trans. Dielectr. Electr. Insul, vol. 13, pp. 862-869, Aug 2006.

[5] IEC 60815, Guide for the selection and dimensioning of high-voltage insulators for polluted conditions - Part 1: Definitions, information and general principles, 2008.

[6] G. Zhicheng, M. Yingke, W. Liming, L. Ruihua, W. Hua, and M. Yi, "Leakage Current and Discharge Phenomenon of Outdoor Insulators", International Journal on Electrical Engineering and Informatics, vol. 1.1, 2009.

[7] G. Haifeng, J. Zhidong, M. Yingke, G. Zhicheng, and W. Liming, "Effect of Hydrophobicity on Electric Field Distribution and Discharges Along Various Wetted Hydrophobic Surfaces", IEEE Trans. Dielectr. Electr. Insul, vol. 15, pp. 435-443, 2008.

[8] S. M. Gubanski, A. Dernfalk, J. Andersson, and H. Hillborg, "Diagnostic Methods for Outdoor Polymeric Insulators", IEEE Trans. Dielectr. Electr. Insul, vol. 14, pp. 1065-1080, 2007.

[9] I. J. Seo, J. Y. Koo, J. K. Seong, B. W. Lee, Y. J. Jeon, and C. H. Lee, "Experimental investigation on the DC breakdown of silicone Polymer composites employable to 500kV HVDC insulator", 1st International Conference on Electric Power Equipment - Switching Technology (ICEPE-ST), pp. 697-700, 2011

[10] S. Y. Teo, H. A. Illias, N. Mokhtar, H. Mokhlis, and A. H. A. Bakar, "Flashover voltage of insulator string under various conditions", IEEE Conf. Power and Energy (PECon) , pp. 119-122, 2014.

[11] S. Kharkovsky and R. Zoughi, "Microwave and millimeter wave nondestructive testing and evaluation - Overview and recent advances", IEEE Instrum. Meas. Mag. vol. 10, pp. 26-38, 2007.

[12] Y. Jiang, S. G. McMeekin, A. J. Reid, A. Nekahi, M. D. Judd, and A. Wilson, "Monitoring Insulator Contamination Level under Dry Condition with a Microwave Reflectometer", International Conference on the Properties and Applications of Dielectric Materials (ICPADM), Sydney, Australia, July 19-22, 2015.

[13] H. Mercier and J. J. Laurin, "A free-space reflectometer for surface impedance measurement of materials in the Ku-band", IEEE

International Symposium on Electromagnetic Compatibility, pp. 62-67. 1995.

[14] D. K. Ghodgaonkar, V. V. Varadan, and V. K. Varadan, "A free-space method for measurement of dielectric constants and loss tangents at microwave frequencies", IEEE Trans. Instrum. Meas. vol. 38, pp. 789-793, 1989.

[15] D. K. Ghodgaonkar, V. V. Varadan, and V. K. Varadan, "Free-space measurement of complex permittivity and complex permeability of magnetic materials at microwave frequencies", IEEE Trans. Instrum. Meas. vol. 39, pp. 387-394, 1990.

[16] IEC 60507, artificial pollution tests on high-voltage insulators to be used on a.c. systems, 1991.

[17] Y. Jiang, S. G. McMeekin, A. J. Reid, A. Nekahi, M. D. Judd, and A. Wilson, "Theoretical Model of Applying Radiometry to Monitor Insulator Containimation", International Conference on Condition Monitoring and Diagnostics (CMD2014), Jeju, Korea, 2014.

[18] Y. Jiang, S. G. McMeekin, A. J. Reid, A. Nekahi, M. D. Judd, and A. Wilson, "High Voltage Insulator Contamination Level Monitoring with X-Band Microwave Radiometer", 23rd International Conference on Electricity Distribution (CIRED2015), Lyon, France, June 15-18, 2015.

[19] A. Stogryn, "Equations for Calculating the Dielectric Constant of Saline Water (Correspondence)", IEEE Trans. Microw. Theory Techn, vol. 19, pp. 733-736, 1971.

[20] J J. A. Lane and J. A. Saxton, "Dielectric Dispersion in Pure Polar Liquids at Very High Radio Frequencies. III. The Effect of Electrolytes in Solution", Mathematical and Physical Sciences, vol. 214, pp. 531-545, 1952.

[21] Y. Lasne, P. Paillou, A. Freeman, T. Farr, K. C. McDonald, G. Ruffie, et al., "Effect of Salinity on the Dielectric Properties of Geological Materials: Implication for Soil Moisture Detection by Means of Radar Remote Sensing", IEEE Trans. Geosci. Remote Sens., vol. 46, pp. 1674-1688, 2008.

[22] M. C. Dobson, F. T. Ulaby, M. T. Hallikainen, and M. A. El-Rayes, "Microwave Dielectric Behavior of Wet Soil-Part II: Dielectric Mixing Models", IEEE Trans. Geosci. Remote Sens., vol. GE-23, pp. 35-46, 1985.

[23] L. Yujiri, M. Shoucri, and P. Moffa, "Passive millimeter wave imaging", IEEE Microwave Magazine, vol. 4, pp. 39-50, 2003.

[24] C. Shu, K. N. Nguyen, and M. N. Afsar, "Complex Dielectric Permittivity Measurements of Glasses at Millimeter Waves and Terahertz Frequencies", 36th European Microwave Conference, pp. 384-387, 2006.

[25] H. E. Bussey and J. E. Gray, "Measurement and Standardization of Dielectric Samples", IRE Transactions on Instrumentation vol. I-11, pp. 162-165, 1962.

Yan Jiang (M'13) was born in Jiangsu, China. He received the B.Sc. degree from Southeast University in Nanjing, China in 2009, the M.Sc. degree in The University of Manchester, UK in 2011. He is now a Ph.D. student in Glasgow Caledonian University. His research interests focus on the development of novel sensors and condition monitoring system for outdoor insulation.

Scott McMeekin is a Professor in the School of Engineering and Built Environment at Glasgow Caledonian University. He received a BSc degree from The University of Strathclyde in 1985 and the MSc and PhD degrees from The University of Glasgow in 1986 and 1989 respectively. Prior to joining Glasgow Caledonian University he was the Process Development manager at Alcatel Optronics Ltd (formerly Kymata Ltd) where he was responsible for the development and qualification of novel optical components for advanced optical telecommunication systems. He has previously worked at the Universities of Cardiff and Glasgow. His current research interests include the development of Instrumentation and Sensor Systems with a specific interest in the condition monitoring of energy assets and the development of photonic bio-sensors. He has published over 110 journal and conferences articles and is co-inventor on 6 patents.

Alistair J. Reid (M'11) graduated from the University of Strathclyde, UK, in 2004 with a B.Eng. (Hons) Degree in Electrical and Mechanical Engineering and received the Ph.D. Degree in 2007 for research on partial discharge monitoring. He conducted post-doctoral research within the Institute for Energy and Environment at the University of Strathclyde from 2007-2011, studying advanced radiometric techniques for partial discharge detection and diagnostic monitoring. In 2011 he gained a 2 year Research Fellowship at Glasgow Caledonian University, UK, and in 2013 was awarded a Visiting Research position at California Institute of Technology's Department of Computing and Mathematical Sciences. He is presently a Lecturer within the School of Engineering and Built Environment at Glasgow Caledonian University conducting research on novel condition monitoring systems.

Azam Nekahi received the B.Sc. degree in electrical engineering from the Amirkabir university of technology (Tehran's Polytechnic) in 2004. She obtained the Master and Ph.D. degrees, respectively in 2007 and 2011 at the Université du Québec à Chicoutimi; within the NSERC/Hydro-Quebec/UQAC Industrial Chair on Atmospheric Icing of Power Network Equipment (CIGELE). Currently Dr. Nekahi is an assistant professor at Glasgow Caledonian University. Her main research interests include outdoor insulation, partial discharge and spectroscopy.

Martin D. Judd (M'2002–SM'2004) is the Technical Director of High Frequency Diagnostics Ltd. He was born in Salford, England in 1963 and graduated from the University of Hull in 1985 with a first class (Hons) degree in Electronic Engineering, after which he gained 8 years of industrial experience, first with Marconi Electronic Devices and then with EEV Ltd. Martin received his PhD from the University of Strathclyde in 1996 for research into the excitation of UHF signals by partial discharges in gas insulated switchgear. He has worked extensively on UHF partial discharge location techniques for power transformers and was latterly Professor of High Voltage Technologies at the University of Strathclyde, where he managed the High Voltage Research Laboratory. In 2014 he founded High Frequency Diagnostics, a contracting and consultancy business that works in partnership with companies and universities to maximize the impact of R&D outputs by utilizing them in new technologies and applications.

Alan Wilson (BSc., PhD, CEng, FIET). After 35 years working in research and technology areas for UK Utilities, CEGB and National Grid, he worked for a further 15 years for Doble Engineering Co in USA, UK and Germany before retiring in 2015. His utility activities included research in dielectrics, management of transformer and cables technology teams and research programme management. More recent work has included strategy management and responsiblity for a subsidiary company in Germany. With well over 100 publications he has been active with IET and CIGRE.